

Particle Acceleration in Relativistic Current Sheets

J. G. Kirk*

Max-Planck-Institut für Kernphysik, Saupfercheckweg 1, D-69117 Heidelberg, Germany

(Received 22 December 2003; published 5 May 2004)

Relativistic current sheets have been proposed as the sites of dissipation in pulsar winds, jets in active galaxies, and other Poynting flux dominated flows. It is shown that the steady versions of these structures differ from their nonrelativistic counterparts because they do not permit transformation to a de Hofmann–Teller frame with zero electric field. Instead, their generic form is that of a true neutral sheet with no linking magnetic field component normal to the sheet. The maximum energy to which such structures can accelerate particles is derived, and used to compute the maximum frequency of the subsequent synchrotron radiation. This can be substantially in excess of standard estimates. In the magnetically driven gamma-ray burst scenario, acceleration of electrons is possible to energies sufficient to enable photon-photon pair production after an inverse Compton scattering event.

DOI: 10.1103/PhysRevLett.92.181101

PACS numbers: 95.30.Qd, 52.27.Ny, 98.54.Cm, 98.70.Rz

Energy release by the process of magnetic reconnection has been suggested as the mechanism responsible for the production of energetic particles in the jets associated with active galactic nuclei (AGN) [1–6] and in pulsar winds [7–11]. It is thought that the same process may also be at work in gamma-ray bursts [12–16]. Reconnection has a large plasma physics, solar physics, and magnetospheric physics orientated literature, that is well summarized in two recent monographs [17,18]. But the physical conditions in the high energy astrophysics applications mentioned above are significantly different, because relativistic effects are important.

In this Letter, it is shown that the generic form of a stationary, relativistic current sheet is that of a true neutral sheet. Typical boundary conditions permit the sheet to be very extended along the magnetic field direction, but a simple argument limits the extent in the direction perpendicular to both the sheet normal and magnetic field vectors. This finding is used to estimate the maximum possible energy to which particles can be accelerated by the dc electric field of the sheet. The results are applied to pulsar winds, gamma-ray bursts, and jets from active galactic nuclei, all of which may contain a magnetically powered relativistic outflow. It is shown that the commonly used estimate of the maximum frequency of synchrotron radiation emitted by an accelerated electron $h\nu \lesssim 100$ MeV can be substantially exceeded when Poynting flux dominates the energy flow.

The current sheets at which reconnection and particle acceleration takes place in astrophysics are relativistic in two senses: First, the magnetization parameter, σ [defined in Eq. (1)], is large and the Alfvén speed $v_A = c\sqrt{\sigma}/(1 + \sigma)$ is close to c . Second, the geometry of the current sheet at which magnetic energy is dissipated is dictated by a highly relativistic plasma flow. Particle acceleration depends crucially on both the magnetization parameter and the field configuration. However, most analytic treatments utilize nonrelativistic models of current sheets. Numerical simulations of current sheets with

$\sigma \approx 1$ have been performed using a two-dimensional particle-in-cell code [19], but the field geometry was constrained to be close to the standard Sweet-Parker configuration. Analytic work on relativistic reconnection [11,20–22] has not yet addressed the question of particle acceleration.

The relativistic effects associated with a large magnetization parameter are readily appreciated. On the other hand, the geometrical effects of a relativistic flow are more subtle. The situation is closely analogous to that of MHD shock fronts, which can be classified into “subluminal” and “superluminal” according to whether the speed of the intersection point of the magnetic field and the shock front is less or greater than c [23,24]. In each case, a Lorentz transformation enables the shock to be viewed from a reference frame in which it has a particularly simple configuration.

Subluminal shocks permit a transformation to a de Hofmann–Teller frame, where the electric field vanishes both upstream and downstream. Nonrelativistic shocks, at which the speed β_{up} of the shock front in units of c observed in the upstream medium is small, $\beta_{\text{up}} \ll 1$, are subluminal, provided the angle between the magnetic field direction and the shock normal in this frame θ_{up} satisfies $\cos\theta_{\text{up}} > \beta_{\text{up}}$. Fine tuning of the upstream magnetic field direction would be required to violate this condition and, given that no MHD wave mode can race ahead of the shock front, this seems unlikely.

On the other hand, the simplest configuration for a superluminal shock is one in which the magnetic field lines are perpendicular to the shock normal both upstream and downstream—an exactly “perpendicular” shock. This is the usual configuration for shocks which are relativistic, i.e., those with $\Gamma = (1 - \beta_{\text{up}}^2)^{-1/2} \gg 1$. Then, fine tuning of the upstream magnetic field direction such that $\sin\theta < 1/\Gamma$ would be needed to avoid superluminal speed of the intersection point.

Thus, the generic nonrelativistic shock can be pictured as a stationary surface crossed by magnetic field lines

along which the plasma flows. The generic relativistic shock, however, can be seen as a stationary surface through which a magnetic field orientated precisely perpendicular to the surface normal is advected by the plasma.

To understand the analogy with current sheets, it is best to consider a specific example: the relativistic MHD wind driven by a pulsar—a rotating neutron star in which a magnetic dipole is embedded with axis oblique to the rotation axis. Approximating the dipole by a split monopole, an asymptotic solution is available, valid at large distance from the star [25]: the wind pulls out the field lines into a striped pattern [26], of wavelength $2\pi\beta r_L$ ($r_L = c/\Omega$ is the light-cylinder radius, Ω the rotation speed of the star) that propagates radially at a speed βc close to c . Figure 1 shows the equatorial plane where a thin helical current sheet separates regions of magnetic field that emerge from opposite magnetic poles. This is the most widely discussed scenario for a pulsar wind, although no solution exists connecting it to realistic boundary conditions at the stellar surface and alternative pictures involving currents which do not collapse into thin sheets have also been proposed [27]. In ideal MHD, the current sheet is a neutral sheet in which the magnetic field vanishes. The inset in Fig. 1 shows that field line reconnection implies a finite “linking” field component perpendicular to the sheet. The term “reconnection” can be misleading here, since the field line configuration is stationary in the corotating frame. However, plasma certainly leaves these field lines, so that the process qualifies as reconnection under a more general definition [18,28].

At a large distance $r \gg r_L$ from the star, the sheet can be considered as locally plane. Then the linking component is in the z direction, and the reversing component in the $\pm x$ direction. The idealized steady reconnection picture discussed here implies an electric field E_y in the y

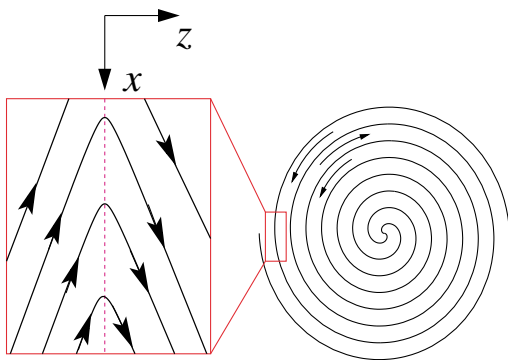


FIG. 1 (color online). The striped pattern of a pulsar wind. A magnetic dipole embedded in the star at an oblique angle to the rotation axis introduces field lines of both polarities into the equatorial plane. The current sheet separating these regions is shown. In the inset, an almost planar portion of this sheet (dashed line) is shown, together with the magnetic field lines, assuming they undergo reconnection.

direction that causes the magnetized plasma to drift into the current sheet from both positive and negative z . A shearing component of the magnetic field in the y direction can also be added, but this vanishes in the equator if the magnetic and rotational axes are orthogonal and will be ignored here, in which case the electric field remains along the y axis.

In a stationary flow, reconnection balances the rate at which magnetic flux is drawn out from the star, implying that the point at which a given magnetic field intersects the current sheet must corotate. However, far from the star, at $r \gg r_L$, the corotation velocity is large compared to c and the relativistic configuration of Fig. 1 implies a drift speed in the sheet that is formally superluminal: $E_y/B_z \gg 1$. This same situation also arises in the case of extragalactic jets, provided they have zero net poloidal flux, i.e., they draw out magnetic flux from a central object [1]. In contrast, the current sheets usually considered in laboratory, solar, and magnetospheric applications are assumed to be of finite length in the x direction and to have subluminal drift speeds at their edges.

A two-dimensional, stationary configuration has E_y constant and, for simplicity, it is usual to assume B_z is constant too. Then it is possible to simplify the fields by performing a Lorentz boost: a subluminal sheet can be transformed by a boost in the x direction at speed cE_y/B_z into the “de Hofmann–Teller” frame in which the electric field vanishes. In this frame the orbits are complex, some being trapped in the sheet and others escaping along the magnetic field lines after one or more passages through the plane $z = 0$. This is the standard configuration for the study of orbits in nonrelativistic current sheets [29,30]. The particle energy is a constant of motion, since $\mathbf{E} = 0$, and no acceleration results unless an additional scattering process is invoked. It is then easy to see that in any other reference frame the acceleration process can be regarded as one of reflection off the magnetic field structure anchored in the sheet. This implies that ions are accelerated more efficiently than electrons, as observed in, for example, the geomagnetic tail [31].

Superluminal sheets, on the other hand, are transformed by a boost along x with speed cB_z/E_y into a configuration with vanishing linking field B_z , but finite E_y . (This is, in fact, a true neutral sheet: the field configuration originally used by Speiser [32] to discuss the orbits of nonrelativistic particles.) In this case all trajectories are trapped in the sheet and acceleration in the $\pm y$ direction ensues, according to the sign of the charge, as soon as a particle drifts into the acceleration zone around $z = 0$, where $|E_y/B_x| > 1$.

Particle acceleration in current sheets with finite B_z has been extensively investigated [33], but the vanishing of B_z has important implications. Most discussions of reconnection treat a Sweet-Parker or Petschek configuration in which the length of the current sheet in the x direction

determines the dissipation rate. The linking field B_z is then crucial for the determination of the spectrum of accelerated particles, and, especially, the maximum permitted energy [5,6], since it is responsible for ejection of particles from the acceleration zone (see also [19]). However, relativistic current sheets, such as that illustrated in Fig. 1 can extend over large distances in the x direction, depending on the nature of the boundary conditions, and the linking field plays no role in ejecting particles. Instead, acceleration in a relativistic sheet is controlled by its finite extent in the direction parallel to the electric field E_y . This is limited not by the boundary conditions, but by local parameter values, as described by Alfvén [34] and Vasylunas [35].

The maximum energy to which a particle can be accelerated by the dc field in a relativistic current sheet is determined by the product of the electric field E_y and the maximum extent Δy in the y direction of the sheet. Alfvén showed that $E_y \times \Delta y$ must be finite by observing that charged particles which drift into the sheet through a surface of area $\Delta x \times \Delta y$ must leave it in opposite directions along the y axis. The current I_y in the y direction, part of which could be carried also by particles entering the sheet along this axis, must therefore exceed the rate of inflow through $\Delta x \times \Delta y$ times the particle charge. Ampère's law, which relates the strength of the reversing component of the field to the current I_y leads to the condition $|qE_y|\Delta y < B_x^2/(4\pi n_\pm)$, where n_\pm is the number density of particles of charge q outside the sheet. This argument, originally limited to stationary sheet configurations, can also be applied to evolving ones [35].

The magnetization parameter σ can be defined in the local plasma rest frame as the ratio of the magnetic enthalpy density to the particle enthalpy density (including rest-mass) w :

$$\sigma = \frac{B^2}{4\pi w}. \quad (1)$$

This quantity equals the ratio of the Poynting flux to the kinetic energy flux of a cold plasma observed in a reference frame moving perpendicular to the magnetic field direction. Assuming the plasma consists of cold electrons and positrons, and that $\sigma \gg 1$, the maximum Lorentz factor γ_{\max} after acceleration is, following Alfvén,

$$\gamma_{\max} = 2\sigma, \quad (2)$$

whereas a cold electron-proton plasma gives

$$\gamma_{\max} \approx \sigma \quad \text{for protons,} \quad (3)$$

$$\gamma_{\max} \approx \sigma M/m \quad \text{for electrons,} \quad (4)$$

with M and m the proton and electron masses, respectively. It is interesting to note that in a plasma in which the magnetic field and particle *rest mass* are in rough equipartition ($\sigma \approx 1$), the upper limit given by Eq. (4) co-

incides with that quoted by Lesch and Birk [2]. However, this situation arises only in relativistic plasmas. In the interstellar medium, for example, $\sigma \approx 10^{-9}$ or smaller, in which case the upper limit on the energy gain reduces to Mv_A^2 . Standard estimates of the interstellar magnetic field and particle density ($1 \mu\text{G}$, $1 \text{ proton}/\text{cm}^3$) imply that electrons can be accelerated, at most, to only mildly relativistic energies. In this case, and in solar system applications, direct acceleration by the dc field may be masked by particle acceleration in the turbulence fed by reconnection or the associated shocks [36].

In addition to the limit imposed by finite Δy , radiative loss processes suffered during acceleration may also affect the maximum particle (and especially electron) energy. In the absence of a linking magnetic field component, the particle trajectories, as first found in the non-relativistic limit by Speiser [32], are attracted to the acceleration zone around the $z = 0$ plane, where they undergo essentially one-dimensional acceleration in the electric field. In this case the losses by synchrotron radiation (or, more precisely, radiation caused by the electromagnetic fields of the sheet) are unimportant. For large σ , this enables synchrotron photons of relatively large energy $h\nu_{\max} \approx (\hbar e B/mc)\gamma_{\max}^2$ to be generated when the accelerated particles leave the current sheet after traversing the distance Δy . This can substantially exceed the frequently quoted (and magnetic field independent) upper limit of $h\nu_{\max} \approx 100 \text{ MeV}$ obtained by setting the synchrotron cooling rate equal to the inverse of the gyro period. For example, a relativistic current sheet in the wind of the Crab pulsar just outside the light-cylinder ($B \approx 10^6 \text{ G}$, $\sigma \approx 10^4$ [11]) is capable of accelerating electrons which subsequently emit synchrotron photons of energy up to 50 GeV, providing a plausible production mechanism [8] for the flux of GeV gamma rays observed by the Energetic Gamma-Ray Experiment Telescope experiment [37].

Unlike synchrotron radiation, inverse Compton scattering on an ambient radiation field is not suppressed for linearly accelerated particles, and can limit the maximum energy, especially near a luminous source such as an AGN. Parametrizing the accelerating electric field by $\eta = |E_y/B_x| < 1$, this limit can be written for a current sheet embedded in a jet that emerges from the AGN with bulk Lorentz factor $\Gamma = \Gamma_{10}/10$ as

$$\gamma_{\max} \approx 10^5 (\eta L_{P47})^{1/4} (\Gamma_{10} R_{12} / L_{bb47})^{1/2}, \quad (5)$$

where L_{P47} and L_{bb47} are the luminosity carried by Poynting flux in the jet and the luminosity of the central photon source, respectively, in units of $10^{47} \text{ erg s}^{-1}$, and $R = 10^{12} R_{12} \text{ cm}$ is the distance of the sheet from this source. Equation (5) assumes that the Compton scattering takes place in the Thomson limit, which is valid for $\gamma_{\max} \lesssim 10^5 \Gamma$.

In the physical conditions thought prevalent at the photosphere of a magnetically accelerated gamma-ray burst outflow [16] ($L_{P47} \approx 10^3$, $L_{bb47} \approx 50$, and $\Gamma \approx 100$ at the photosphere $R = 10^{11}$ cm), Eq. (5) indicates a maximum electron Lorentz factor (in the co-moving frame) of $\gamma_{\max} \approx 4 \times 10^5$. However, since the photon field in this case has a relatively high temperature (≈ 1 keV), we conclude that Compton scattering is unable to limit the maximum electron energy to a value such that the Thomson limit applies, and, consequently, that photon-photon pair creation is likely to ensue. A feedback mechanism appears possible here, since pair creation will depress the magnetization parameter σ , and, hence, the limit given by Eq. (2).

Relativistic current sheets are known to be unstable to the growth of the tearing mode [38] and other instabilities are also likely to operate (see, for example, [39]). On scale lengths comparable to the sheet thickness it is likely that an oscillating component of B_z will be generated. As discussed in standard nonrelativistic pictures, this may, on small scales, cause breakup of the sheet into a series of magnetic islands and X points arranged alternately along the x axis, providing stochastic deflections of the particle trajectories within the sheet. Such a scattering mechanism is, in fact, essential for the formation of an equilibrium structure such as the Harris sheet [40], and it may also play a role in enhancing the effect of synchrotron losses. However, in a steady relativistic sheet the boundary conditions do not permit this scattering process to evacuate the plasma from the dissipation region, because they prevent the formation of a stationary pattern with outflow along the x axis. On the other hand, a quasi-stationary pattern containing relativistic sheets of finite extent in the y direction does appear possible, and enables estimates of the maximum permitted energy of particles accelerated by the dc field to be made. In reality, relativistic sheets may dissipate in a highly nonstationary fashion as suggested in the nonrelativistic case by, for example, solar observations [36], but clarification of this must await the results of numerical simulations of the generic relativistic sheet configuration.

I thank Y. Lyubarsky for helpful comments on the manuscript.

*Electronic address: John.Kirk@mpi-hd.mpg.de

- [1] M. M. Romanova and R. V. E. Lovelace, *Astron. Astrophys.* **262**, 26 (1992).
- [2] H. Lesch and G. T. Birk, *Astron. Astrophys.* **324**, 461 (1997).
- [3] H. Lesch and G. T. Birk, *Astrophys. J.* **499**, 167 (1998).
- [4] H. Wiechen, G. T. Birk, and H. Lesch, *Phys. Plasmas* **5**, 3732 (1998).
- [5] Y. E. Litvinenko, *Astron. Astrophys.* **349**, 685 (1999).
- [6] D. A. Larrabee, R. V. E. Lovelace, and M. M. Romanova, *Astrophys. J.* **586**, 72 (2003).
- [7] F. C. Michel, *Comments Astrophys. Space Phys.* **3**, 80 (1971).
- [8] Y. Lyubarskii, *Astron. Astrophys.* **311**, 172 (1996).
- [9] Y. Lyubarsky and J. G. Kirk, *Astrophys. J.* **547**, 437 (2001).
- [10] J. G. Kirk, O. Skjæraasen, and Y. A. Gallant, *Astron. Astrophys.* **388**, L29 (2002).
- [11] J. G. Kirk and O. Skjæraasen, *Astrophys. J.* **591**, 366 (2003).
- [12] C. Thompson, *Mon. Not. R. Astron. Soc.* **270**, 480 (1994).
- [13] H. C. Spruit, *Astron. Astrophys.* **341**, L1 (1999).
- [14] H. C. Spruit, F. Daigne, and G. Drenkhahn, *Astron. Astrophys.* **369**, 694 (2001).
- [15] G. Drenkhahn, *Astron. Astrophys.* **387**, 714 (2002).
- [16] G. Drenkhahn and H. C. Spruit, *Astron. Astrophys.* **391**, 1141 (2002).
- [17] E. R. Priest and T. Forbes, *Magnetic Reconnection* (Cambridge University Press, Cambridge, 2000).
- [18] D. Biskamp, *Magnetic Reconnection in Plasmas* (Cambridge University Press, Cambridge, 2000).
- [19] S. Zenitani and M. Hoshino, *Astrophys. J.* **562**, L63 (2001).
- [20] E. G. Blackman and G. B. Field, *Phys. Rev. Lett.* **72**, 494 (1994).
- [21] M. Lyutikov and D. Uzdensky, *Astrophys. J.* **589**, 893 (2002).
- [22] M. Lyutikov, *Mon. Not. R. Astron. Soc.* **346**, 540 (2003).
- [23] L. O. Drury, *Rep. Prog. Phys.* **46**, 973 (1983).
- [24] M. C. Begelman and J. G. Kirk, *Astrophys. J.* **353**, 66 (1990).
- [25] S. V. Bogovalov, *Astron. Astrophys.* **349**, 1017 (1999).
- [26] F. V. Coroniti, *Astrophys. J.* **349**, 538 (1990).
- [27] J. Kuijpers, *Pub. Astron. Soc. Aust.* **18**, 407 (2001).
- [28] M. Hesse and K. Schindler, *J. Geophys. Res.* **93**, 5559 (1988).
- [29] J. Büchner and L. M. Zelenyi, *J. Geophys. Res.* **94**, 11821 (1989).
- [30] J. Chen, *J. Geophys. Res.* **97**, 15011 (1992).
- [31] L. A. Daglis, S. Livi, E. T. Sarris, and B. Wilken, *J. Geophys. Res.* **99**, 5691 (1994).
- [32] T. W. Speiser, *J. Geophys. Res.* **70**, 4219 (1965).
- [33] S. I. Syrovatskii, *Annu. Rev. Astron. Astrophys.* **19**, 163 (1981).
- [34] H. Alfvén, *J. Geophys. Res.* **73**, 4379 (1968).
- [35] V. M. Vasylunas, *J. Geophys. Res.* **85**, 4616 (1980).
- [36] P. J. Cargill, *Adv. Space Res.* **26**, 1759 (2001).
- [37] P. L. Nolan *et al.*, *Astrophys. J.* **409**, 697 (1993).
- [38] L. M. Zelenyi and V. V. Krasnosel'skikh, *Astron. Zh.* **56**, 819 (1979).
- [39] W. Daughton, *Phys. Plasmas* **6**, 1329 (1999).
- [40] E. G. Harris, *Nuovo Cimento* **23**, 115 (1962).